Gut Microbial Utilization of the Alternative Sweetener, D-Allulose, via AlsE

Authors:

Glory Minabou Ndjite[1], Angela Jiang[1,2], Charlotte Ravel[1], Maggie Grant[1], Xiaofang Jiang[2], Brantley Hall[1,3*]

Affiliations:

[1]College of Computer, Mathematical and Natural Sciences, University of Maryland, College Park, Maryland, USA

[2]National Library of Medicine, National Institutes of Health, Bethesda, Maryland, USA

[3]Center for Bioinformatics and Computational Biology, University of Maryland, College Park, College Park, Maryland, USA

[*]Corresponding author: brantley@umd.edu

Abstract

D-allulose, a rare sugar with emerging potential as a low-calorie sweetener, has garnered attention as an alternative to other commercially available alternative sweeteners, such as sugar alcohols, which often cause severe gastrointestinal discomfort. D-allulose-6-phosphate 3-epimerase (AlsE) is a prokaryotic enzyme that converts D-allulose-6-phosphate into D-fructose-6-phopshate, enabling its use as a carbon source. However, the taxonomic breadth of AlsE across gut bacteria remains poorly understood, hindering insights into the utilization of D-allulose by microbial communities. In this study, we provide experimental evidence showing that *Clostridium innocuum* is capable of D-allulose metabolism via a homologous AlsE. A bioinformatics search of 85,202 bacterial genomes identified 116 bacterial species with AlsE homologs, suggesting a limited distribution of AlsE in bacteria. Additionally, *Escherichia coli* contains a copy of *alsE*, but it does not grow on D-allulose as a sole carbon source unless *alsE* is heterologously expressed. A metagenomic analysis revealed that 15.8% of 3,079 adult healthy human metagenomic samples that we analyzed contained *alsE*, suggesting a limited prevalence of the enzyme in the gut microbiome. These results suggest that the gut microbiome has limited capacity to metabolize D-allulose via *alsE*, supporting its use as an alternative sweetener with minimal impact on microbial composition and gastrointestinal symptoms. This finding also enables personalized nutrition, allowing diabetic individuals to assess their gut microbiota for *alsE*, and manage glycemic response while reducing gastrointestinal distress.

Introduction

The obesity epidemic is a serious health issue affecting many countries worldwide.[1] According to the National Health and Nutrition Examination Survey (NHANES), conducted by the National Center for Health Statistics (NCHS), 41.9% of U.S. adults aged 20 and older are obese.[2] As an individual's amount of adipose tissue increases, so too does their risk for metabolic diseases, including type 2 diabetes,[3] which is caused by insulin resistance and lack of insulin, resulting in chronic hyperglycemia.[4] Over 415 million people worldwide suffer from diabetes, over 90% of whom have type 2 diabetes.[5] In the U.S., 14.8% of adults aged 20 or older are also affected.[2]

Previous studies have linked increased sugar consumption to the obesity and diabetes epidemic.[6,7] Further, researchers propose that a high-carbohydrate diet promotes the deposition of calories into fatty tissue, leading to weight gain through increased hunger.[8] The main culprits of type 2 diabetes are excessive sugar consumption and a sedentary lifestyle.[5] There is no cure for type 2 diabetes available as of 2024, and much more research is needed on methods to mitigate and prevent diabetes, including decreasing the consumption of fructose, glucose, and sucrose.

One potential strategy to minimize sugar consumption is to use sugar substitutes, such as aspartame, sucralose, erythritol, xylitol, and sorbitol.[9] These alternative sweeteners tend to taste sweet, but the human body does not metabolize them, thereby reducing the adverse health effects of excess sugar consumption.[10] These sweeteners may be derived from plant extracts or from chemical synthesis.[11]

Many of the alternative sweeteners currently approved by the U.S. Food and Drug Administration include sugar alcohols and non-nutritive sweeteners (NNS), both of which

have been associated with some side effects on the human gut microbiome. Sugar alcohol consumption can lead to gastrointestinal discomfort and have laxative effects through osmotic pressure and increased gas production through gut bacterial fermentation, resulting in diarrhea and bloating.[12] Moreover, increased blood erythritol levels have been associated with increased platelet reactivity, resulting in cardiovascular events such as strokes.[13] On the other hand, regular NNS consumption can lead to functional alteration of gut microbiota composition, resulting in an impaired glycemic response and glucose intolerance.[14,15] Therefore, it is extremely important to understand the mechanisms of how alternative sweeteners interact with the human gut microbiome. These findings have led to an increasing interest in fructose epimers, sugar molecules that resemble fructose but have altered stereochemistry at one carbon atom.[16] One example is D-allulose (also known as D-psicose), a rare low-calorie sweetener that is the C-3 epimer of fructose and is found in small amounts in certain fruits.[16] Previous studies have suggested that D-allulose has a low glycemic index, making it promising for reducing the risk of diabetes.[17–20] Due to advances in the industrial process and bacterial engineering methods, D-allulose production is becoming increasingly economically viable.[21] Thus, D-allulose is a promising way to decrease sucrose and fructose consumption.

Although D-allulose is a promising alternative sweetener, its side effects are poorly understood compared to other types of alternative sweeteners. A significant portion of ingested D-allulose reaches the gut microbiome, as approximately 30% passes through the small intestine unabsorbed and is excreted in feces[22,23]. While 70% of D-allulose is absorbed via glucose transporter type 5 (GLUT5) in the small intestine, the substantial

unabsorbed fraction has the potential to interact with and impact the gut microbial community.[22,23] Studies in murine models have shown that D-allulose can induce changes in the gut microbiome.[24,25] Comparatively, Suez et al. 2014 showed that saccharin, sucralose, and aspartame can induce glucose intolerance through modifications of the gut microbiome composition and function.[26] Therefore, there is an urgent need to better understand both the potential for D-allulose utilization by gut bacteria and its effects on human gut microbiome composition.

Some bacteria possess the ability to metabolize D-allulose using the enzyme D-allulose-6-phosphate 3-epimerase (AlsE), encoded by the gene *alsE*.[27] In *E. coli* K-12, *alsE* is in the D-allose operon, which has been well characterized (**Figure 1A**).[28] First, D-allose is converted into D-allulose 6-phosphate via AlsK and RpiB. Then, AlsE catalyzes the reversible conversion of D-allulose 6-phosphate to D-fructose 6-phosphate.[29] Environmental and clinical isolates of *Klebsiella pneumoniae,* an opportunistic pathogen responsible for a significant number of nosocomial bacterial infections,[30] are capable of metabolizing D-allulose using a homologous AlsE, raising concerns that consuming D-allulose may confer opportunistic pathogens an advantage in colonization.[31,32] However, there has not been a full systematic annotation of the prevalence and distribution of *alsE* in the human gut microbiome.

To address this gap, we combined bioinformatic predictions and experimental verification to characterize the distribution of *alsE* in human gut microbes. Our bioinformatic predictions were validated through growth experiments, culturing bacteria in media with D-allulose as the sole carbon source. Our investigation of multiple representatives of the major gut bacterial clades expanded the known phylogenetic range

of D-allulose metabolism from phylum Pseudomonadota to include phylum Bacillota by identifying that *Clostridium innocuum* 6_1_30 is capable of using D-allulose as a sole carbon source. Through comparative genomics and protein homology searches, we identified a putative AlsE in *C. innocuum* that is homologous to AlsE in *K. pneumoniae* (35% identity, e-value 2.89e-41) that has a divergent operon organization compared to the known D-allulose metabolizers. We verified the function of the *C. innocuum* AlsE in the *E. coli* Keio Knockout Collection, observing that *E. coli* deficient in native *alsE* was able to grow on D-allulose when complemented with *C. innocuum alsE*. We also found that *E. coli*, despite encoding *alsE*, cannot grow on D-allulose as a sole carbon source unless *alsE* is heterologously expressed. To comprehensively characterize the taxonomic distribution of AlsE, we performed a systematic search across 85,202 bacterial genomes, identifying 116 species encoding putative *alsE* homologs. The limited distribution of *alsE* in the gut microbiome supports D-allulose's promise as an alternative sweetener with minimal impact on both microbial composition and gastrointestinal symptoms, two common drawbacks of current artificial sweeteners. Although our focus is on *alsE*, it is important to note that there could be alternative undiscovered pathways bacteria can use to metabolize D-allulose that our study did not cover. These findings provide insights into bacterial D-allulose metabolism, supporting its development as an alternative sweetener to help reduce sugar consumption in the context of rising rates of obesity and diabetes.

Results

Investigating the potential for D-allulose utilization by gut microbes

To identify gut bacterial species capable of utilizing D-allulose as a carbon source, we conducted a preliminary identification of species with D-allulose-6-phosphate 3-

epimerase (AlsE) homologs by conducting a BLASTp search against 85,202 non-redundant genomes from the Genome Taxonomy Database[33,34]. We used the experimentally verified *Klebsiella pneumoniae* AlsE as the query, with a threshold of 50% identity and bitscore greater than 200. There were 272 species that met the threshold, mostly from non-gut bacteria. Some gut bacteria genera with AlsE homologs include *Klebsiella*, *Escherichia*, and *Clostridium*. Interestingly, *Clostridium innocuum*, a common gut bacterium species, contained an AlsE hit (50.49% identity, 2.30e-77 e-value, 220 bitscore).

To experimentally validate our bioinformatic predictions and characterize D-allulose metabolism across diverse gut bacteria, we tested representative strains from major gut bacterial phyla including Bacillota, Bacteroidota, Actinobacteriota, and Pseudomonadota for growth on D-allulose as a sole carbon source (**Figure 2A**). Growth was quantified by spectrophotometric measurement at OD600, with significant growth defined as a three-fold increase in OD600 compared to media negative controls. *Clostridium innocuum* 6_1_30 demonstrated robust growth on D-allulose with a 6:1 ratio in its OD600 measurement compared to the media blank, revealing a previously unknown metabolic capability (**Figure 2B**). Notably, *Escherichia coli* DC10B did not grow on D-allulose despite encoding *alsE* within its D-allose operon (**Figure 2C**), prompting further investigation.

Escherichia coli* does not readily utilize D-allulose *in vitro* despite encoding *alsE

Although *E. coli* encodes *alsE* within the D-allose operon (*alsRBACEK*), previous studies have demonstrated that this operon is specifically induced in response to D-

allose.[28] We hypothesized that while *E. coli* encodes the metabolic machinery for D-allulose utilization; this capability may not be active in the absence of D-allose.

To test this hypothesis, we placed *alsE* under the control of an IPTG-inducible promoter to enable controlled expression independent of its native regulation. Using the Keio collection, a comprehensive library of single-gene knockout mutants in *E. coli* BW25113[35], we cloned the *alsE* gene from strain JW2760 into a pCW-lic vector backbone under an inducible *tac* promoter, creating the pCW-lic-*E.coli alsE* construct. This plasmid was transformed into the Keio *alsE* knockout strain, and the transformed bacteria were cultured in M9 minimal media supplemented with D-allulose and IPTG.[12]

Our results showed that both the Keio *alsE* knockout and the untransformed *E. coli* were unable to grow using D-allulose as the sole carbon source. In contrast, the transformed *E. coli* overexpressing *alsE* exhibited robust growth (**Figure 3A and 3B**). These findings support our hypothesis that while *E. coli* encodes AlsE, it may not be capable of utilizing D-allulose as a carbon source in the absence of D-allose.

Limited distribution of *alsE* across *E. coli* strains

We then investigated the presence and absence of *alsE* across *E. coli* genomes, using a previously published pangenome consisting of 1,324 *E. coli* genomes.[36] *alsE* was present in 598 out of 1324 *E. coli* genomes (45%), suggesting that *alsE* is a strain-specific gene and may not be present in every individual's gut microbiome, despite the prevalence of *E. coli* exceeding 90% among in humans.[37]

Identification of *alsE* in *Clostridium innocuum*

Given that *Clostridium innocuum* 6_1_30 grew on D-allulose as a sole carbon source, we investigated the genomic origins of its D-allulose metabolism. Based on our prior preliminary search results, we hypothesized that a homologous *alsE* was responsible for D-allulose metabolism in *C. innocuum* rather than a novel pathway. To conduct a comprehensive search for AlsE homologs in *C. innocuum*, we used the *Klebsiella pneumoniae* MGH 78578 AlsE (NCBI accession: GCA_000016305.1) as the query to search the *C. innocuum* genome (NCBI accession: GCA_000183585.2). BLASTp revealed two AlsE homologs in *C. innocuum*, referred to as ci04257 and ci04568 (ci04257: 50.49% identity, 2.09e-76 e-value; ci04568: 35% identity, 2.89e-41 e-value). We examined the gene neighborhood of the two *alsE* candidates. The neighborhood of ci04257 consisted mainly of genes encoding hypothetical proteins. On the other hand, ci04568 was adjacent to phosphotransferase systems (PTS), which could potentially perform the phosphorylation and import step of D-allulose utilization. In addition, the neighboring genes are annotated with sugar metabolism functions, such as fructose bisphosphate aldolase. Therefore, we hypothesized that ci04568 encodes an enzyme that possibly performs a similar function to AlsE. Interestingly, the putative *alsE* gene neighborhood in *C. innocuum* is completely divergent from the *alsE* gene neighborhood in other species known to metabolize D-allulose, such as *Klebsiella pneumoniae* (**Figure 1B**).[31] Of note, this putative *alsE* was a core gene present in all 283/283 available *C. innocuum* genomes on NCBI, with all of them containing a nearly identical, if not identical, homolog to *alsE* in 6_1_30.

We then sought to functionally validate the candidate *alsE* in *C. innocuum* by cloning the gene into a pCW-lic vector backbone under an inducible tac promoter, resulting in the pCW-lic_C.inn_*alsE* construct to heterologously express *C. innocuum's alsE* in *E. coli* (**Supplemental Figure 1**). The plasmid was then transformed into the Keio collection *E. coli alsE* knockout. The transformed bacteria were subsequently inoculated in D-allulose-supplemented M9 and induced *alsE*'s expression using IPTG.[12] The Keio *alsE* knockout demonstrated no growth on D-allulose, while complementation of the *C. innocuum* gene into the knockout restored function, resulting in growth on D-allulose (**Figure 3C and 3D**).

Few Gut Bacterial Species Encode AlsE

Once we experimentally verified the function of the *C. innocuum* and *E. coli* AlsE, we used ProkFunFind,[38] a bioinformatics pipeline to systematically search for AlsE in bacteria. We used the experimentally verified AlsE protein sequences from *K. pneumoniae* MGH 78578, *C. innocuum* 6_1_30, and *E. coli* K-12 as queries to search the 85,202 non-redundant prokaryotic genomes from the Genome Taxonomy Database (GTDB) for species that contained homologs to AlsE. We used a more stringent filtering criteria compared to the preliminary search, filtering hits based on a 30% identity threshold and a maximum e-value of 1e-100. Our search revealed 116 putative bacterial species with AlsE (**Supplemental Table 3**, **Figure 4**). The vast majority of these species were from the phylum Pseudomonadota (103/116), 10 were from the phylum Bacillota, and 3 were from Fusobacteriota. Out of those 116 species, only 35 are known to be part of the animal gut microbiota. Some known members of the human gut microbiome with AlsE include *Klebsiella oxytoca*, *Enterobacter cloacae*, and *Serratia marcescens*. Other

species with AlsE that are not gut-associated are primarily isolated from plants and soil, including *Klebsiella planticola*,[39] *Rahnella aquatilis*,[40] and members of the *Kosakonia* genus.[41,42] Of note, none of the species that were unable to grow on D-allulose during our initial investigation contained AlsE homologs, with the exception of *Escherichia coli* as discussed before (*Bacteroides cellulosilytious*, *Lactobacillus reuteri*, *Clostridium symbiosum*, *Bifidobacterium adolescentis*, *Ruminococcus gnavus*).

Presence of *alsE* in the healthy adult gut microbiome

To investigate the prevalence of *alsE* in the human gut microbiome, we examined the presence and absence of *alsE* in 3,079 healthy adult human gut microbiomes that passed quality checks. We built a reference database using both experimentally characterized and bioinformatically discovered *alsE*, with thresholds of 30% identity and 1e-100 e-value. We then aligned healthy adult human stool metagenomic reads downloaded from SRA to our *alsE* reference database and normalized the alignment counts into counts per million. To strike a balance between spurious hits and sensitivity, we considered any metagenomes with at least 1 count per million to contain *alsE*. 488 out of 3,079 metagenomes met our threshold for *alsE* presence, approximately 15.8%.

Delineation of AlsE from Pentose-5-Phosphate 3-Epimerase

In order to elucidate the evolutionary origins of AlsE, we used a combination of phylogenetic analyses, ancestral state reconstruction, and sequence conservation. Using eggNOG-mapper (v6.0), we determined that AlsE belonged to the orthologous group COG0036 (pentose-5-phosphate 3-epimerase). We constructed a phylogenetic tree using the top 1,323 homologs of the 3 experimentally verified AlsE protein sequences against all COG0036 sequences. Based on branch lengths and the presence of the

238 experimentally verified AlsE, we identified a putative AlsE clade that contains 515
239 sequences. We were able to identify conserved amino acid changes in the putative AlsE
240 node from the ancestral node (**Figure 5A**), such as from G52 to S52, V134 to Y134, L142
241 to T142, and an N147 to D147 **(Figure 5B)**. Based on the high entropy in the alignment
242 at these positions, these are conserved changes and may differentiate AlsE from other
243 pentose-5-phosphate 3-epimerases.

244 To determine putative catalytic residues, we performed a structural alignment of
245 the AlphaFold2-predicted structure of *C. innocuum* AlsE to the crystal structure of *E. coli*
246 AlsE (pdb: 3CT7). Based on the active site residues reported by Chan et al. 2008 in *E.*
247 *coli* AlsE, we determined that the putative active site residues in both *Clostridium*
248 *innocuum* and *Klebsiella pneumoniae* are similar based on the structural alignment
249 (**Figure 5C**).[29] In *C. innocuum*, these putative residues are His 32, Asp 35, His 66, and
250 Asp 175, which align to His 34, Asp 36, His 67, and Asp 176 in *E. coli*, respectively.
251 Therefore, despite being distant homologs, *C. innocuum* likely shares similar catalytic
252 residues to *E. coli* AlsE.

Discussion

Many widely used commercial alternative sweeteners, such as sugar alcohols, are associated with significant gastrointestinal discomfort.[12] This discomfort arises from the malabsorption of these sweeteners, leading to osmotic diarrhea, and from fermentation by gut microbes, which produce gas.[12] Consequently, there is an urgent need to identify alternative sweeteners, such as D-allulose, that do not cause gastrointestinal symptoms.

The presence of gut bacteria that can potentially metabolize D-allulose via D-allulose-6-phosphate 3-epimerase (AlsE) has significant implications for its use as a commercial alternative sweetener. Prior to our study, while D-allulose metabolism had been identified in some human gut bacteria, there had not been a systematic analysis of the presence, abundance, and distribution of enzymes involved in D-allulose metabolism across gut bacterial species - a knowledge gap that limited our understanding of how gut bacteria utilize this sweetener. In our study, we demonstrated that *Clostridium innocuum* can metabolize D-allulose through a homologous AlsE by examining its growth on D-allulose media. These findings shed light on the role of the gut microbiome in D-allulose metabolism.

During the initial investigation for gut microbial species capable of growing on D-allulose as a sole carbon source, *C. innocuum* 6_1_30 grew on D-allulose as a sole carbon source while *E. coli* was unable to grow despite encoding *alsE* in its genome, which was intriguing. Past studies have shown that despite *E. coli* having *alsE* in its genome, its expression was too weak to support the production of D-allulose from D-fructose without genetic modifications.[21,43] This is consistent with our findings that the *E. coli* only grew on D-allulose when *alsE* was heterologously expressed, verified via the

insertion of the respective *alsE* genes into the Keio *alsE* knockout mutant, which resulted in *E. coli* gaining the ability to use D-allulose as a sole carbon source.

Our findings show that AlsE protein homologs are only present in a few gut bacterial species. Out of 85,202 bacterial genomes from the GTDB, only 116 bacterial species were annotated to contain AlsE homologs. Our finding that *E. coli* cannot grow on D-allulose without heterologously expressing *alsE* suggests that some of these 116 species may not be able to metabolize D-allulose effectively. In addition, only 35 of these species are known to be present in animal gut microbiomes. These data suggest that D-allulose utilization might be restricted to a small number of species within the human gut microbiome. This finding is in alignment with the scarcity of D-allulose in nature. D-allulose has only been found in small quantities in a few plant species, such as *Itea virginica* and wheat.[44,45] Moreover, several of the bacterial species with putative *alsE* were primarily isolated from plants such as wheat or maize, including *Klebsiella planticola*,[39] *Rahnella aquatilis*,[40] and members of the *Kosakonia* genus.[41,42] We speculate that D-allulose metabolism may confer a metabolic advantage for these bacteria that live in plant-associated habitats, where exposure to D-allulose is more likely. Alternatively, *alsE* may have evolved primarily to confer D-allose metabolism, with D-allulose metabolism being incidental.

Notably, the limited presence of *alsE* in gut microbiome species suggests that D-allulose may serve as a valuable alternative to common sugar substitutes, which are known to cause gastrointestinal discomfort and alter microbiome composition. Previous studies have reported that D-allulose can be consumed in relatively high doses, up to 0.5 g/kg body weight, without causing significant gastrointestinal issues.[46] Thus, the limited

metabolism of D-allulose by gut bacteria, combined with its low impact on gastrointestinal function, suggests that it may offer a promising solution for individuals seeking low-calorie sweeteners without adverse digestive effects. Of note, approximately 15.8% of human metagenomes analyzed contained *alsE*, suggesting that individual gut microbiomes may respond differently to D-allulose consumption. Diabetic individuals looking to cut their glucose consumption may benefit from individual microbiome testing to choose the alternative sweetener that is less likely to be utilized by their gut microbiome.

Our study focuses on AlsE as an enzyme responsible for D-allulose metabolism, though we recognize the possibility of alternative mechanisms of D-allulose metabolism. To our knowledge, AlsE is the only currently known enzyme implicated in D-allulose metabolism in bacteria. However, there may be alternative mechanisms of bacterial D-allulose metabolism that are undiscovered, given the limited studies on the subject.[28,31] Due to this possibility of unknown alternative mechanisms, we cannot be certain of D-allulose's impact on gut microbiome composition at large.

In conclusion, we shed light on the taxonomic distribution of AlsE in the gut microbiota. We discovered that *C. innocuum* is capable of growing on D-allulose as a sole carbon source. In addition, while *E. coli* has *alsE*, it cannot grow on D-allulose without heterologously expressing *alsE*, suggesting that many of these bacteria do not necessarily grow on D-allulose as a sole carbon source. A relatively small fraction of gut microbes are capable of utilizing D-allulose, making it a promising alternative to commercially available sugar substitutes, such as sugar alcohols.

Methods

Identification of D-allulose-6-phosphate 3-epimerases in the GTDB genomes: All representative genomes from the Genome Taxonomy Database (GTDB) (release r207) were downloaded, and protein sequences for each genome were predicted using Prokka (version 1.14.6).[34,47] The *Escherichia coli* K-12, *Klebsiella pneumoniae* MGH78578, and *Clostridium innocuum* 6_1_30 D-allulose-6-phosphate 3-epimerase protein sequences were searched against 85,202 reference genomes using the ProkFunFind pipeline (v0.1.0).[38] The hits were filtered based on an 1e-100 e-value and 30% identity thresholds, resulting in putative 126 AlsE amino acid sequences from 116 nonredundant genomes.

Phylogenetic analyses: Sequences from the GTDB assigned to COG0036 were identified using eggNOG-mapper (version 2.1.3).[48] A BLASTp search was conducted (version 2.15.0+) using the identified D-allulose 6-phosphate 3-epimerases as queries against these identified sequences, setting a limit to the top 1,305 hits. Sequence alignment was performed using Clustal Omega (version 1.2.4).[49,50] Columns that have more than 97% gaps were removed to enhance alignment quality using Goalign (version 0.3.7).[51] Phylogenetic analysis was carried out using IQ-TREE (version 2.1.2) with default parameters and model selection[52]. The reliability of the phylogenetic trees was evaluated using 1,000 ultrafast bootstrap replicates. Trees were visualized using the Interactive Tree Of Life (iTOL).[53]

Ancestral sequence reconstruction was performed on the AlsE tree using GRASP (version 04-May-2023), with default parameters.[54] We then manually inspected the tree to delineate AlsE from other Pentose-5-phosphate 3-epimerases. We calculated the

343 entropy of the alignments using Goalign via the compute pssm function (v.0.3.7).[51] The
344 figures were created using the Python package logomaker (v0.08).[55]
345
346 *Growth of anaerobic bacteria:* Bacterial strains were acquired from the NIH Biodefense
347 and Emerging Infections Research Resources Repository (BEI). Each strain was
348 inoculated from a glycerol stock and grown under anaerobic conditions over a 24-hour
349 period at 37 °C in an anaerobic chamber (Coy Laboratory Products) in Brain-Heart
350 Infusion (BHI) broth (Research Products International, B11000) supplemented with
351 glucose. 25 µL of the culture was inoculated into 4 mL of minimal media (M9)
352 supplemented with 10 mg/mL carbon source (glucose or D-allulose).[12]
353
354 *Absorbance Assay:* The transformed Keio Δ*alsE*::*C. Innocuum alsE* & Keio Δ*alsE*::*E. coli*
355 *alsE* constructs were shaken in Luria-Bertani (LB) supplemented with 100 µg/mL
356 carbenicillin (GoldBio, C-103-25) overnight at 37°C. 25 µL of the overnight culture was
357 inoculated in 4 mL triplicates of minimal media (M9) supplemented with 100µM Isopropyl
358 β- d-1-thiogalactopyranoside (IPTG, GoldBio, I2481C25), 100 µg/mL carbenicillin, 50
359 µg/mL kanamycin (Bio Basic, KB0286), and 10 mg/mL D-allulose[12] (Chem-Impex,
360 32353). For kinetic measurements, 250 µL of the triplicates were aliquoted into a 96-well
361 acrylic, clear bottom plate (Celltreat, 229592), sealed with a Breathe Easy membrane
362 (Electron Microscopy Sciences, 70536-10), and incubated at 37°C for 48-70 hours
363 depending on the strain observed. The end-point absorbance at 600 nm was measured
364 with a Spectramax M5 plate reader, with end-point bacterial growth calculated using a
365 ratio to the blank, with a ratio of 3 indicating significant growth.

366

367 *pCW-lic_C.inn_alsE & pCW-lic-E.coli_alsE constructs:* In order to achieve ectopic
368 expression of *alsE* from *Clostridium innocuum* 6_1_30 and *E. coli* JW2760[35] in the
369 knockout mutants, the *alsE* gene was amplified and cloned into the pCW-lic vector
370 backbone (Addgene, 26098). Genomic DNA from *C. innocuum* and *E. coli* JW2760 was
371 utilized in a polymerase chain reaction (PCR) using Phusion High-Fidelity DNA
372 Polymerase (NEB, M0530S) with the specific primers listed in Supplementary Table 1. A
373 Monarch PCR & DNA Cleanup Kit (NEB, T1030S) was used to purify the amplified
374 product. The pCW-lic vector backbone was digested with restriction enzymes NdeI (NEB,
375 R0111S) and HindIII-HF (NEB, R3104S), followed by purification with a Monarch PCR &
376 DNA Cleanup Kit. A Gibson assembly was completed using Gibson Assembly Master Mix
377 (NEB, E2611S) in accordance with the manufacturer's instructions. The resulting
378 constructs were stored at -20°C until needed for use.

379

380 *Keio-pCW construct:* The *alsE* gene was amplified and cloned into the pCW-lic vector
381 backbone under a tac promoter and transformed into the Keio collection *als*E knockout
382 as detailed above with the same primers outlined in Supplementary Table 1. For the
383 control, an empty pCW-lic vector was cloned into the Keio *alsE* knockout.

384

385 *Chemical competency:* The Keio collection *alsE* knockout was made competent using the
386 Mix & Go! *E. coli* Transformation Kit and Buffer Set (Zymo, T3001) in accordance with the
387 manufacturer's protocol and stored at -80°C until needed for use.

388

389 *Transformation:* Both constructs were independently transformed into the chemically
390 competent Keio collection *alsE* knockout in accordance with the manufacturer's protocol
391 (Zymo, T3001). The resulting transformed cells were plated on LB agar plates
392 supplemented with 100 µg/uL of carbenicillin. Successful transformation was validated
393 via Oxford Nanopore sequencing by Plasmidsaurus.
394
395 *Structural prediction and molecular docking:* The structure for the *Clostridium innocuum*
396 6_1_30 AlsE was predicted using AlphaFold2 (v2.3.0).[56] Binding pockets were predicted
397 using fpocket (v4.0) with default parameters.[57] The pockets were compared to the
398 homologous *Escherichia coli* AlsE (3CT7) to identify putative substrate binding regions
399 and catalytic residues.[29] The structure for D-allulose (PubChem compound identifier:
400 50909805) was docked onto the predicted AlsE structure using AutoDock Vina (v4.2).[58,59]
401 The docking simulation was performed within 15 Å × 15 Å × 15 Å cubes centered on the
402 center points of the chosen fpocket substrate binding pocket with exhaustiveness set to
403 32. Docking results were visualized using PyMOL.[60] We used Foldseek to identify the top
404 structural homolog.[61] The predicted AlsE protein structure was aligned with the *E. coli*
405 3CT7, and the putative catalytic residues were identified based on the previous work by
406 Chan et al. 2008, using TM-Align.[29,62] Protein sequence conservation of AlsE was
407 visualized using ConSurf based on the putative AlsE clade.[63,64]
408
409 *Profiling of alsE presence in the gut:* To build the reference database, we used *alsE*
410 identified by ProkFunFind, which were filtered based on a threshold of e-value 1e-100
411 and percent identity 30%, resulting in a total of 126 sequences. We downloaded a

412 collection of adult healthy metagenomic biosamples that passed basic quality control
413 (n=3410) from SRA, and then trimmed adapters with Trim-Galore with default settings.
414 The reads were then mapped to a human reference (assembly T2T-CHM13v2.0) to
415 identify potential contaminants and removed them using Samtools (v1.16).[65] We removed
416 any samples with less than a million reads after curation, resulting in 3,079 samples, and
417 then aligned the remaining reads to the *alsE* reference database using bowtie2 (v2.4.1).[66]
418 The number of reads mapped to the *alsE* reference was summarized by normalizing the
419 number of reads in the sample and then multiplying by one million to obtain counts per
420 million (cpm). If a biosample had multiple SRRs, we concatenated the read counts and
421 total reads across all SRRs per sample before calculating cpm. We considered samples
422 with at least 1 cpm as containing *alsE*, to account for spurious alignments.
423

424 ## Author Statements

425 **Author contributions:** B.H. and X.J. conceptualized and supervised the project. All
426 authors performed the experiments and analyzed the data. G.M.N, A.J., C.R., and M.G.
427 wrote the original draft of the manuscript. All authors reviewed and edited the paper.
428 **Funding information:** B.H is supported by startup funding from the University of
429 Maryland and NIH grant 1R35GM155208-01. A.J. and X.J. are supported by the
430 Intramural Research Program of the NIH, National Library of Medicine.
431 **Conflicts of interest:** The authors declare that there are no conflicts of interest.
432 **Acknowledgments:** This work utilized the computational resources of the NIH HPC
433 Biowulf cluster (http://hpc.nih.gov) and the UMIACS cluster at the University of Maryland's
434 Center for Bioinformatics and Computational Biology (https://www.umiacs.umd.edu/).

pCW-LIC was a gift from Cheryl Arrowsmith (Addgene plasmid # 26098 ; http://n2t.net/addgene:26098 ; RRID:Addgene_26098)

Data and materials availability: The authors confirm that the data supporting the findings of this study are available within the article and its supplementary materials.

References

1. Phelps, N. H. *et al.* Worldwide trends in underweight and obesity from 1990 to 2022: a pooled analysis of 3663 population-representative studies with 222 million children, adolescents, and adults. *The Lancet* **403**, 1027–1050 (2024).
2. Stierman, B. *et al. National Health and Nutrition Examination Survey 2017 - March 2020 Prepandemic Data Files - Development of Files and Prevalence Estimates for Selected Health Outcomes*. https://stacks.cdc.gov/view/cdc/106273 (2021) doi:10.15620/cdc:106273.
3. Klein, S., Gastaldelli, A., Yki-Järvinen, H. & Scherer, P. E. Why Does Obesity Cause Diabetes? *Cell Metab.* **34**, 11–20 (2022).
4. Mejia, E. & Pearlman, M. Natural Alternative Sweeteners and Diabetes Management. *Curr. Diab. Rep.* **19**, 142 (2019).
5. Chatterjee, S., Khunti, K. & Davies, M. J. Type 2 diabetes. *The Lancet* **389**, 2239–2251 (2017).
6. Ludwig, D. S., Peterson, K. E. & Gortmaker, S. L. Relation between consumption of sugar-sweetened drinks and childhood obesity: a prospective, observational analysis. *Lancet Lond. Engl.* **357**, 505–508 (2001).
7. Bray, G. A., Nielsen, S. J. & Popkin, B. M. Consumption of high-fructose corn syrup in beverages may play a role in the epidemic of obesity. *Am. J. Clin. Nutr.* **79**, 537–543 (2004).

8. Ludwig, D. S. & Ebbeling, C. B. The Carbohydrate-Insulin Model of Obesity: Beyond "Calories In, Calories Out". *JAMA Intern. Med.* **178**, 1098–1103 (2018).

9. Wee, M., Tan, V. & Forde, C. A Comparison of Psychophysical Dose-Response Behaviour across 16 Sweeteners. *Nutrients* **10**, 1632 (2018).

10. Chattopadhyay, S., Raychaudhuri, U. & Chakraborty, R. Artificial sweeteners – a review. *J. Food Sci. Technol.* **51**, 611–621 (2014).

11. Leśniewicz, A., Wełna, M., Szymczycha-Madeja, A. & Pohl, P. The Identity and Mineral Composition of Natural, Plant-Derived and Artificial Sweeteners. *Molecules* **28**, 6618 (2023).

12. Hattori, K. *et al.* Gut Microbiota Prevents Sugar Alcohol-Induced Diarrhea. *Nutrients* **13**, 2029 (2021).

13. Witkowski, M. *et al.* The artificial sweetener erythritol and cardiovascular event risk. *Nat. Med.* **29**, 710–718 (2023).

14. Oku, T. & Nakamura, S. Digestion, absorption, fermentation, and metabolism of functional sugar substitutes and their available energy. *Pure Appl. Chem.* **74**, 1253–1261 (2002).

15. Suez, J. *et al.* Personalized microbiome-driven effects of non-nutritive sweeteners on human glucose tolerance. *Cell* **185**, 3307-3328.e19 (2022).

16. Noronha, J. C. *et al.* The Effect of Small Doses of Fructose and Its Epimers on Glycemic Control: A Systematic Review and Meta-Analysis of Controlled Feeding Trials. *Nutrients* **10**, 1805 (2018).

17. Matsuo, T. & Izumori, K. Effects of Dietary D -Psicose on Diurnal Variation in Plasma Glucose and Insulin Concentrations of Rats. *Biosci. Biotechnol. Biochem.* **70**, 2081–2085 (2006).

18. Franchi, F. *et al.* Effects of D-allulose on glucose tolerance and insulin response to a standard oral sucrose load: results of a prospective, randomized, crossover study. *BMJ Open Diabetes Res. Care* **9**, e001939 (2021).

485 19. Teysseire, F. *et al.* Metabolic Effects and Safety Aspects of Acute D-allulose and
486 Erythritol Administration in Healthy Subjects. *Nutrients* **15**, 458 (2023).
487 20. Braunstein, C. R. *et al.* A Double-Blind, Randomized Controlled, Acute Feeding
488 Equivalence Trial of Small, Catalytic Doses of Fructose and Allulose on Postprandial Blood
489 Glucose Metabolism in Healthy Participants: The Fructose and Allulose Catalytic Effects
490 (FACE) Trial. *Nutrients* **10**, 750 (2018).
491 21. Taylor, J. E. *et al.* Awakening the natural capability of psicose production in Escherichia
492 coli. *Npj Sci. Food* **7**, 54 (2023).
493 22. Iida, T. *et al.* Failure of d-psicose absorbed in the small intestine to metabolize into
494 energy and its low large intestinal fermentability in humans. *Metabolism.* **59**, 206–214 (2010).
495 23. Kishida, K. *et al.* d-Allulose is a substrate of glucose transporter type 5 (GLUT5) in the
496 small intestine. *Food Chem.* **277**, 604–608 (2019).
497 24. Han, Y. *et al.* Alteration of Microbiome Profile by D-Allulose in Amelioration of High-Fat-
498 Diet-Induced Obesity in Mice. *Nutrients* **12**, 352 (2020).
499 25. Han, Y., Yoon, J. & Choi, M.-S. Tracing the Anti-Inflammatory Mechanism/Triggers of d-
500 Allulose: A Profile Study of Microbiome Composition and mRNA Expression in Diet-Induced
501 Obese Mice. *Mol. Nutr. Food Res.* **64**, 1900982 (2020).
502 26. Suez, J. *et al.* Artificial sweeteners induce glucose intolerance by altering the gut
503 microbiota. *Nature* **514**, 181–186 (2014).
504 27. Xia, Y. *et al.* Research advances of D-allulose: An overview of physiological functions,
505 enzymatic biotransformation technologies, and production processes. *Foods* **10**, 2186
506 (2021).
507 28. Kim, C., Song, S. & Park, C. The D-allose operon of Escherichia coli K-12. *J. Bacteriol.*
508 **179**, 7631–7637 (1997).
509 29. Chan, K. K., Fedorov, A. A., Fedorov, E. V., Almo, S. C. & Gerlt, J. A. Structural Basis
510 for Substrate Specificity in Phosphate Binding (β/α)8-Barrels: d-Allulose 6-Phosphate 3-

Epimerase from Escherichia coli K-12. *Biochemistry* **47**, 9608–9617 (2008).

30. Podschun, R. & Ullmann, U. *Klebsiella* spp. as Nosocomial Pathogens: Epidemiology, Taxonomy, Typing Methods, and Pathogenicity Factors. *Clin. Microbiol. Rev.* **11**, 589–603 (1998).

31. Blin, C., Passet, V., Touchon, M., Rocha, E. P. C. & Brisse, S. Metabolic diversity of the emerging pathogenic lineages of Klebsiella pneumoniae. *Environ. Microbiol.* **19**, 1881–1898 (2017).

32. Martin, R. M. *et al.* Identification of Pathogenicity-Associated Loci in Klebsiella pneumoniae from Hospitalized Patients. *mSystems* **3**, e00015-18 (2018).

33. McGinnis, S. & Madden, T. L. BLAST: at the core of a powerful and diverse set of sequence analysis tools. *Nucleic Acids Res.* **32**, W20 (2004).

34. Parks, D. H. *et al.* GTDB: an ongoing census of bacterial and archaeal diversity through a phylogenetically consistent, rank normalized and complete genome-based taxonomy. *Nucleic Acids Res.* **50**, D785–D794 (2022).

35. Baba, T. *et al.* Construction of *Escherichia coli* K-12 in-frame, single-gene knockout mutants: the Keio collection. *Mol. Syst. Biol.* **2**, (2006).

36. Tantoso, E. *et al.* To kill or to be killed: pangenome analysis of Escherichia coli strains reveals a tailocin specific for pandemic ST131. *BMC Biol.* **20**, 146 (2022).

37. Tenaillon, O., Skurnik, D., Picard, B. & Denamur, E. The population genetics of commensal Escherichia coli. *Nat. Rev. Microbiol.* **8**, 207–217 (2010).

38. Dufault-Thompson, K. & Jiang, X. Annotating microbial functions with ProkFunFind. *mSystems* **9**, e00036-24.

39. Bagley, S. T., Seidler, R. J. & Brenner, D. J. Klebsiella planticola sp. nov.: A new species of enterobacteriaceae found primarily in nonclinical environments. *Curr. Microbiol.* **6**, 105–109 (1981).

40. Berge, O. *et al.* Rahnella aquatilis, a nitrogen-fixing enteric bacterium associated with

the rhizosphere of wheat and maize. *Can. J. Microbiol.* **37**, 195–203 (2011).

41. Berger, B. *et al.* Successful Formulation and Application of Plant Growth-Promoting Kosakonia radicincitans in Maize Cultivation. *BioMed Res. Int.* **2018**, 6439481 (2018).

42. Berger, B., Baldermann, S. & Ruppel, S. The plant growth-promoting bacterium Kosakonia radicincitans improves fruit yield and quality of Solanum lycopersicum. *J. Sci. Food Agric.* **97**, 4865–4871 (2017).

43. Guo, Q. *et al.* Metabolically Engineered Escherichia coli for Conversion of D-Fructose to D-Allulose via Phosphorylation-Dephosphorylation. *Front. Bioeng. Biotechnol.* **10**, 947469 (2022).

44. Miller, B. S. & Swain, T. Chromatographic analyses of the free amino-acids, organic acids and sugars in wheat plant extracts. *J. Sci. Food Agric.* **11**, 344–348 (1960).

45. Ayers, B. J. *et al.* Iteamine, the first alkaloid isolated from *Itea virginica* L. inflorescence. *Phytochemistry* **100**, 126–131 (2014).

46. Han, Y. *et al.* Gastrointestinal Tolerance of D-Allulose in Healthy and Young Adults. A Non-Randomized Controlled Trial. *Nutrients* **10**, 2010 (2018).

47. Seemann, T. Prokka: rapid prokaryotic genome annotation. *Bioinformatics* **30**, 2068–2069 (2014).

48. Cantalapiedra, C. P., Hernández-Plaza, A., Letunic, I., Bork, P. & Huerta-Cepas, J. eggNOG-mapper v2: Functional Annotation, Orthology Assignments, and Domain Prediction at the Metagenomic Scale. *Mol. Biol. Evol.* **38**, 5825–5829 (2021).

49. Sievers, F. *et al.* Fast, scalable generation of high-quality protein multiple sequence alignments using Clustal Omega. *Mol. Syst. Biol.* **7**, 539 (2011).

50. Camacho, C. *et al.* BLAST+: architecture and applications. *BMC Bioinformatics* **10**, 421 (2009).

51. Lemoine, F. & Gascuel, O. Gotree/Goalign: toolkit and Go API to facilitate the development of phylogenetic workflows. *NAR Genomics Bioinforma.* **3**, lqab075 (2021).

563 52. Minh, B. Q. *et al.* IQ-TREE 2: New Models and Efficient Methods for Phylogenetic
564 Inference in the Genomic Era. *Mol. Biol. Evol.* **37**, 1530–1534 (2020).
565 53. Letunic, I. & Bork, P. Interactive Tree of Life (iTOL) v6: recent updates to the
566 phylogenetic tree display and annotation tool. *Nucleic Acids Res.* **52**, W78–W82 (2024).
567 54. Leslie, R., O'Donnell, C. J. & Johnson, A. D. GRASP: analysis of genotype-phenotype
568 results from 1390 genome-wide association studies and corresponding open access
569 database. *Bioinforma. Oxf. Engl.* **30**, i185-194 (2014).
570 55. Tareen, A. & Kinney, J. B. Logomaker: Beautiful sequence logos in python. 635029
571 Preprint at https://doi.org/10.1101/635029 (2019).
572 56. Jumper, J. *et al.* Highly accurate protein structure prediction with AlphaFold. *Nature* **596**,
573 583–589 (2021).
574 57. Le Guilloux, V., Schmidtke, P. & Tuffery, P. Fpocket: An open source platform for ligand
575 pocket detection. *BMC Bioinformatics* **10**, 168 (2009).
576 58. Eberhardt, J., Santos-Martins, D., Tillack, A. F. & Forli, S. AutoDock Vina 1.2.0: New
577 Docking Methods, Expanded Force Field, and Python Bindings. *J. Chem. Inf. Model.* **61**,
578 3891–3898 (2021).
579 59. Trott, O. & Olson, A. J. AutoDock Vina: improving the speed and accuracy of docking
580 with a new scoring function, efficient optimization and multithreading. *J. Comput. Chem.* **31**,
581 455–461 (2010).
582 60. PyMOL. [(accessed on 22 July 2024)]. Available online: http://www.pymol.org/pymol.
583 61. van Kempen, M. *et al.* Fast and accurate protein structure search with Foldseek. *Nat.*
584 *Biotechnol.* **42**, 243–246 (2024).
585 62. Zhang, Y. & Skolnick, J. TM-align: a protein structure alignment algorithm based on the
586 TM-score. *Nucleic Acids Res.* **33**, 2302–2309 (2005).
587 63. Ashkenazy, H. *et al.* ConSurf 2016: an improved methodology to estimate and visualize
588 evolutionary conservation in macromolecules. *Nucleic Acids Res.* **44**, W344-350 (2016).

64. Ben Chorin, A. *et al.* ConSurf-DB: An accessible repository for the evolutionary conservation patterns of the majority of PDB proteins. *Protein Sci. Publ. Protein Soc.* **29**, 258–267 (2020).

65. Li, H. *et al.* The Sequence Alignment/Map format and SAMtools. *Bioinformatics* **25**, 2078–2079 (2009).

66. Langmead, B. & Salzberg, S. L. Fast gapped-read alignment with Bowtie 2. *Nat. Methods* **9**, 357–359 (2012).

Figures

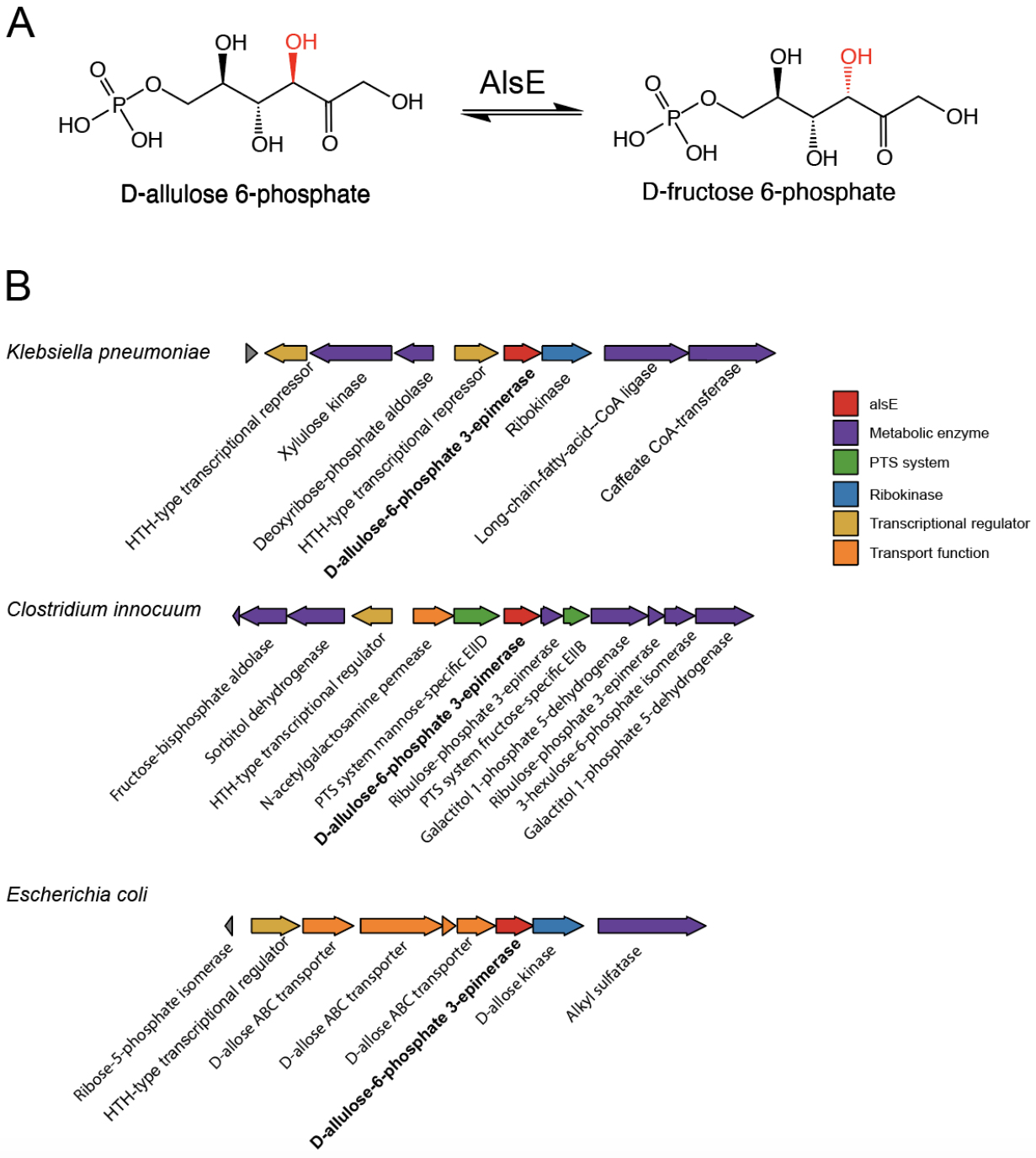

Figure 1: A) Conversion of D-allulose-6-phosphate into D-fructose-6-phosphate by *alsE*. B) *alsE* cluster organization from *Klebsiella pneumoniae* MGH78578, *Clostridium innocuum* 6_1_30, and *Escherichia coli* K-12.

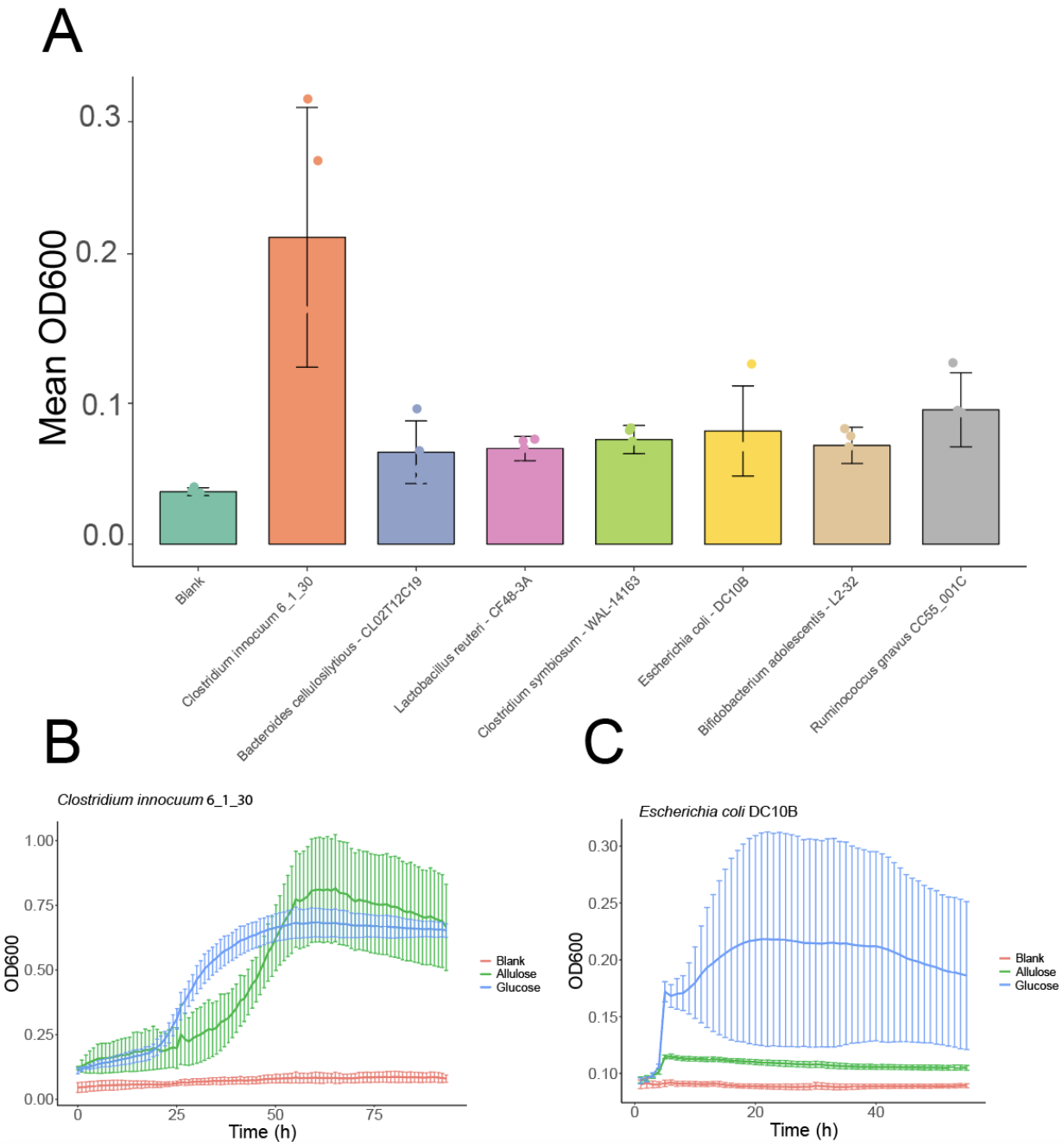

Figure 2: Identification of *Clostridium innocuum* 6_1_30 as a gut bacteria species that can grow on allulose as a sole carbon source. A) Investigation of 7 gut bacteria species (*Clostridium innocuum* 6_1_30, *Bacteroides cellulosilytious* - CL02T12C19, *Lactobacillus reuteri* CF48-3A, *Clostridium symbiosum* WAL-14163, *Escherichia coli* DC10B,

606 *Bifidobacterium adolescentis* L2-32, *Ruminococcus gnavus* CC55_001C) for growth on
607 allulose as the sole carbon source. Each data point is the average of three technical
608 replicates from a single biological replicate per species. B) Growth curve of *C. innocuum*
609 6_1_30 on allulose with minimal media. Allulose is the growth curve of *C. innocuum* when
610 grown on allulose, while Glucose is a positive control of *C. innocuum* growing on glucose,
611 and Blank refers to *C. innocuum* grown on blank media as a negative control. C) Growth
612 curve of *E. coli* DC10B (Col02) on allulose with minimal media.
613

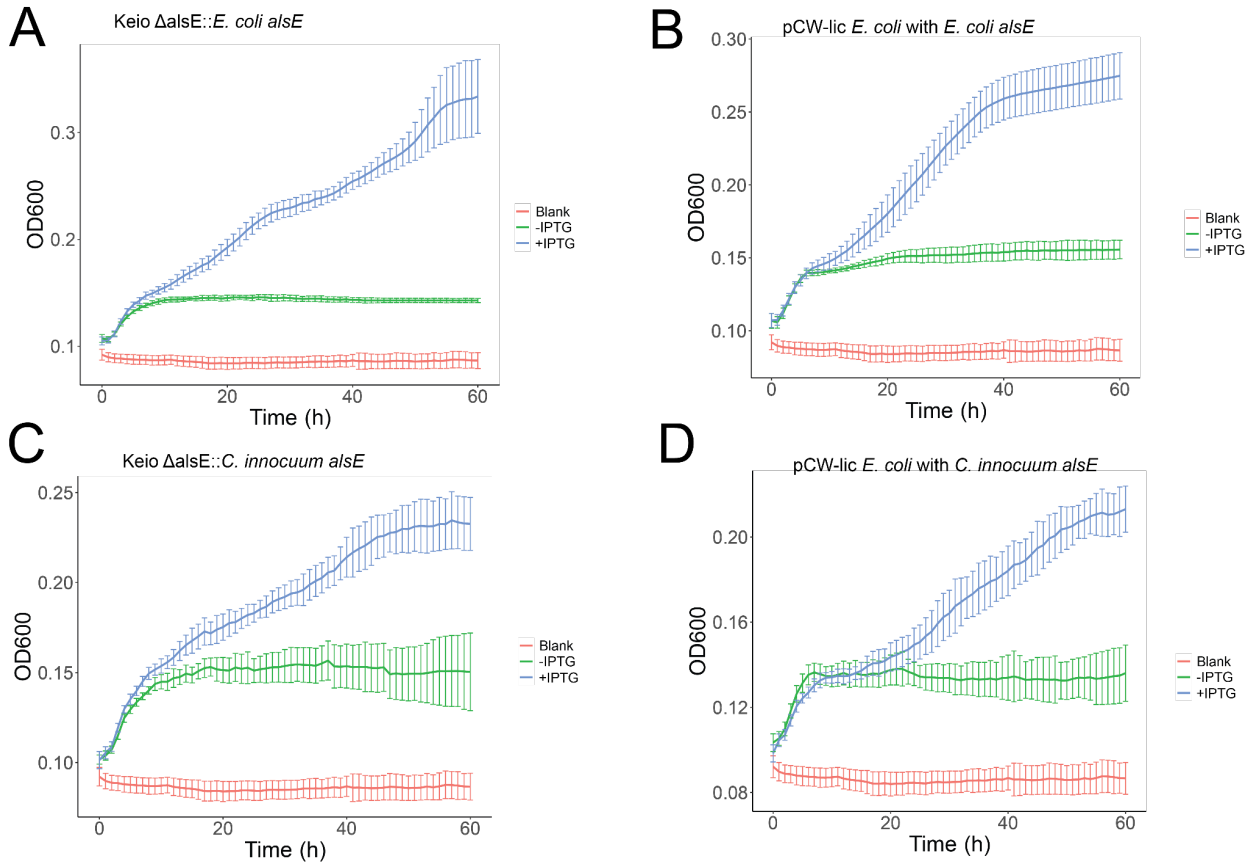

614
615

Figure 3: A and B) Verification of the *Escherichia coli alsE* functionality. Keio Δ*alsE*::*E. coli alsE* + IPTG is the growth curve of the transformed Keio pCW-lic-E.coli_*alsE*, containing the wild-type *E. coli alsE* with IPTG to induce ectopic expression. Keio Δ*alsE*::*E. coli alsE* is the growth curve of the transformed Keio *E. coli* without IPTG, resulting in no gene expression. C and D) Verification of the *Clostridium Innocuum* 6_1_30 *alsE* functionality. Keio Δ*alsE*::*C. Innocuum alsE* + IPTG is the growth curve of the transformed Keio pCW-lic_C.Inn_*alsE*, containing the *C. innocuum alsE* with IPTG to induce ectopic expression. Keio Δ*alsE*::*C. Innocuum alsE* is the growth curve of the same transformed Keio *E. coli* without IPTG, resulting in reduced gene expression.

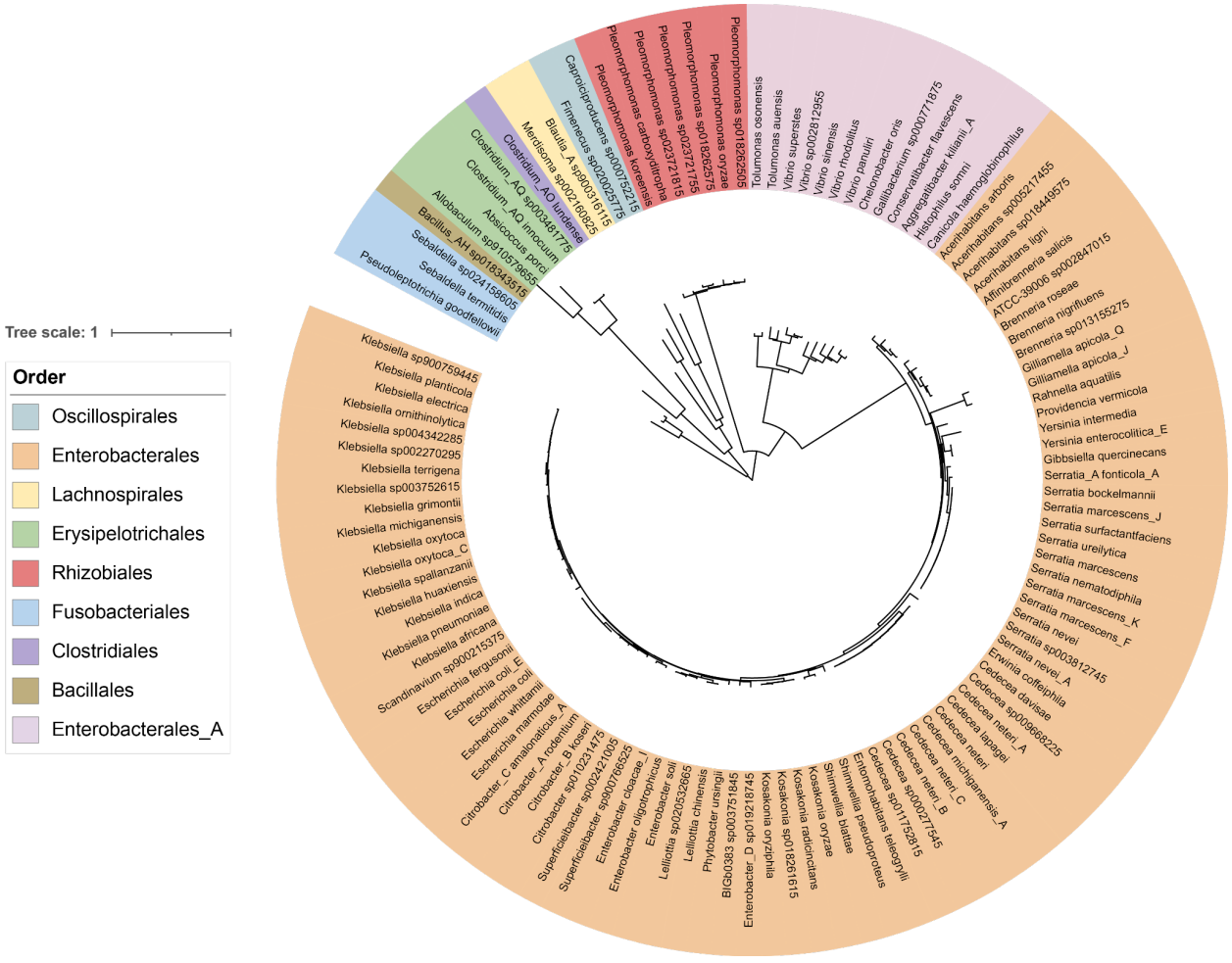

626 **Figure 4:** Species tree showing the taxonomic distribution of AlsE in microbial genomes
627 from GTDB, colored by order. The species tree was generated by pruning the GTDB
628 species tree using the Gotree prune command.[51]
629

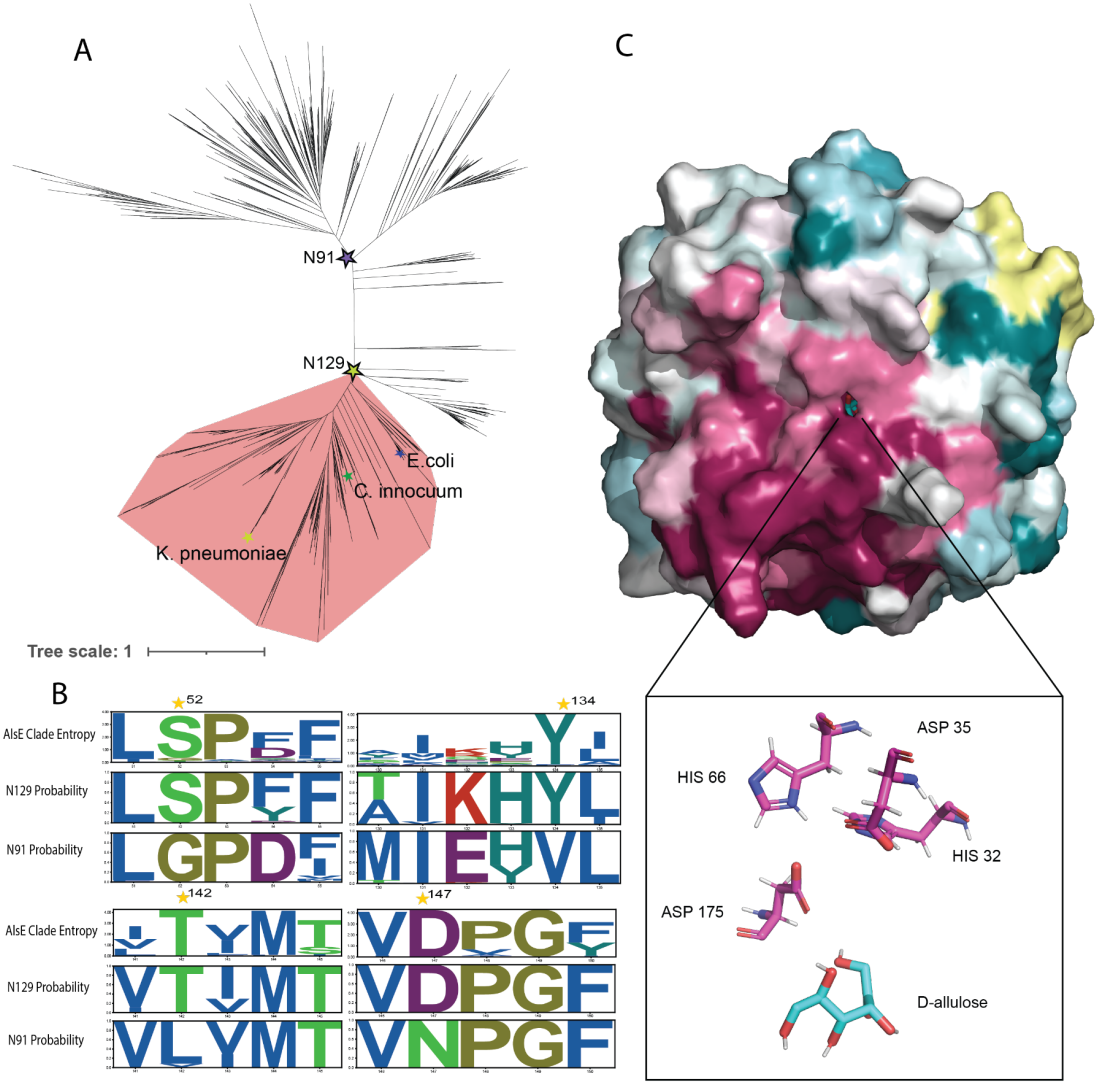

630
631 **Figure 5:** A) Gene tree constructed from putative AlsE sequences and related enzymes
632 annotated as pentose-5-phosphate-3-epimerase (COG0036), showing a possible
633 delineation of the AlsE clade and the location of *Klebsiella pneumoniae*, *Clostridium*
634 *innocuum*, and *Escherichia coli* AlsE. B) Diagram showing the change and conservation

635 (entropy) of residues in the putative AlsE clade, as well as the GRASP predicted ancestral
636 states of N129 (AlsE clade) and N91 (putative ancestral node). Residues with a predicted
637 conserved change from the ancestral state are labeled with a star. C) D-allulose docked
638 to the AlphaFold2-predicted structure of *C. innocuum* 6_1_30 AlsE, colored by amino acid
639 conservation via Consurf.

Supplementary Materials

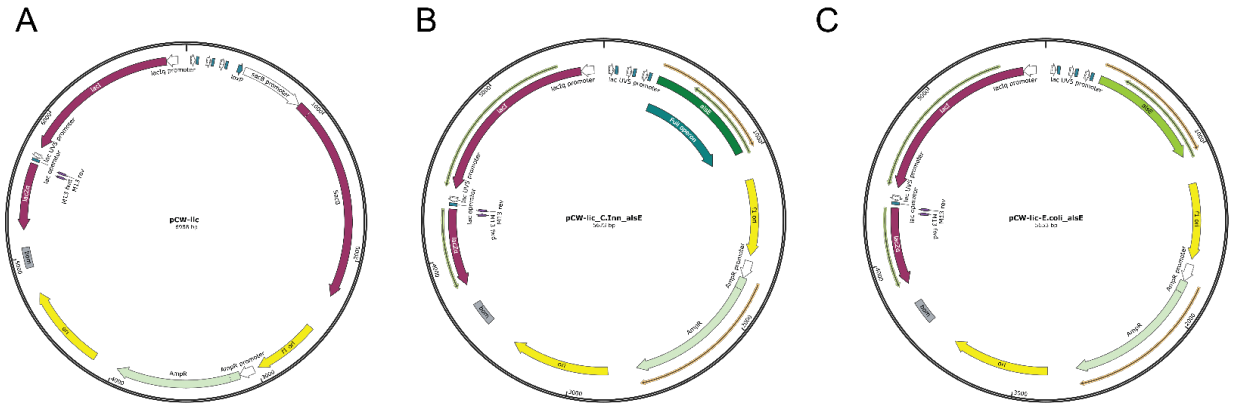

Supplementary Figure S1: Plasmid maps of constructs. A) pCW-lic vector backbone.31 B) pCW-lic_C.inn_*alsE* vector containing the D-Allulose-6-phosphate 3-Epimerase (*alsE*) gene from *C. innocuum* ligated into the pCW-lic vector backbone via Gibson assembly. C) pCW-lic-E.Coli_*alsE* vector containing the *alsE* gene from *E. coli* ligated into the pCW-lic backbone. Pale green arrows represent an ampicillin resistance gene. Maps created using SnapGene.

654 **Supplementary Table 1: Primers used in construct development**

Strain		**Sequence (5' > 3')**
C. innocuum 6_1_30	Forward	CATCGATGCTTAGGAGGTCAAATGGAT ATAAAAATATCACCATCTATC
	Reverse	TTGACAGCTTATCAGCGATATTATTTTTC CAATTCCTGAAC
E. coli JW2760	Forward	CATCGATGCTTAGGAGGTCAAATGAAAA TCTCCCCCTCGTTAATG
	Reverse	TTGACAGCTTATCAGCGATATTATGCTG TTTTTGCATGAGGC

655

656 **Supplementary Table 2:** Predicted AlsE amino acid sequences identified with taxonomy
657 information.

658 **Supplementary Table 3:** Metadata on the metagenomics samples used in this study,
659 including SRA numbers and sample ids, along with the read mapping counts and total
660 reads.